RMetS
Royal Meteorological Society

Stratospheric impact on tropospheric winds deduced from potential vorticity inversion in relation to the Arctic Oscillation

Yvonne Hinssen,* Aarnout van Delden, Theo Opsteegh and Wouter de Geus
Institute for Marine and Atmospheric Research Utrecht, The Netherlands
*Correspondence to: Yvonne Hinssen, Institute for Marine and Atmospheric Research Utrecht, PO Box 80000, 3508 TA Utrecht, The Netherlands. E-mail: y.b.l.hinssen@uu.nl

The zonal mean state of the atmosphere in the Northern Hemisphere in winter is determined by the temperature at the Earth's surface and by two potential vorticity (PV) anomalies (defined as that part of the PV field that induces a wind field) centred over the North Pole: one in the upper troposphere/lower stratosphere (UTLS), extending to the Subtropics, and the other over the polar cap in the lower to middle stratosphere. Isentropic PV inversion demonstrates that the UTLS PV anomaly induces the main part of the zonal mean wind in the troposphere, including the subtropical jet stream, while the stratospheric PV anomaly induces the polar night stratospheric jet. The stratospheric PV anomaly has a greater amplitude and extends further downwards if the Arctic Oscillation (AO) index is positive. Also, the UTLS PV anomaly has a slightly larger amplitude if the AO index is positive, but the meridional PV gradient in the Subtropics that is associated with this anomaly is greatest when the AO index is negative, resulting in a stronger subtropical jet when the AO index is negative. PV inversion translates the UTLS PV anomaly into a wind anomaly and a static stability anomaly. The resulting differences in the vertical wind shear and in the Brunt–Väisälä frequency between the two AO phases show a larger baroclinicity in the extratropics when the AO index is positive. This explains why more extratropical cyclones are observed when the AO index is positive. Copyright © 2010 Royal Meteorological Society

Key Words: stratosphere–troposphere coupling; invertibility principle; static stability; vertical wind shear

Received 29 July 2008; Revised 3 September 2009; Accepted 14 October 2009; Published online in Wiley InterScience

Citation: Hinssen Y, van Delden A, Opsteegh T, de Geus W. 2010. Stratospheric impact on tropospheric winds deduced from potential vorticity inversion in relation to the Arctic Oscillation. *Q. J. R. Meteorol. Soc.*

1. Introduction

Research over the past decade has shown that the stratosphere can have an important influence on surface climate (Hartley *et al.*, 1998; Baldwin and Dunkerton, 1999, 2001; Black, 2002; Ambaum and Hoskins, 2002). Many studies indicate a relation between the strength of the stratospheric polar vortex and the phase of the Arctic Oscillation (AO), a dominant pattern of natural climate variability at the Earth's surface in the mid- to high latitudes of the Northern Hemisphere in winter (Thompson and Wallace, 1998). A positive AO index is in general positively correlated with a stronger stratospheric polar vortex (Hartmann *et al.*, 2000; Thompson and Wallace, 1998, 2000).

In the present article, we adhere to the idea sketched by Ambaum and Hoskins (2002) that a positive North Atlantic Oscillation (NAO) index (an index strongly related to the AO index) is associated with a positive stratospheric potential vorticity (PV) anomaly over the Pole (compared with the climatological average), because of more equatorward refraction of upward-propagating Rossby waves and therefore less mixing of PV over the Pole by wave breaking. Ambaum and Hoskins (2002)

use regression techniques and scale analysis based on PV dynamics to estimate the effect of a stratospheric PV anomaly on the tropopause, and subsequently on the surface pressure.

The present study is also related to the work of Black (2002), who examined the stratospheric forcing of the zonal mean surface winds associated with the AO for winter mean conditions. Black used quasi-geostrophic piecewise PV inversion to study the contribution of stratospheric PV anomalies on the tropospheric wind field. Here we use a PV inversion equation that is based on the nonlinear isentropic PV. Therefore, in contrast to Black (2002), we take variations of the static stability with latitude into account. This is an important aspect of the response of the atmosphere to a PV anomaly, especially, as we shall see, in the upper troposphere and lower stratosphere (UTLS).

Furthermore, whereas Black (2002) defines a PV anomaly as an anomaly with respect to the climate, we follow Hoskins *et al.* (1985) by defining a PV anomaly as that part of the PV field that induces a wind field according to the solution of the PV inversion equation. With this definition we are able to distinguish very clearly two separate PV anomalies centred over the Pole: one at the tropopause and the other in the polar night stratosphere above about 425 K. The former PV anomaly was not identified as such by Black (2002).

Following the ideas of Davis (1992) about piecewise PV inversion, we examine the effect of the two separate PV anomalies on the zonal mean zonal wind in the troposphere for episodes of positive and negative AO index in January. The month of January is chosen because the correlation between the stratospheric polar PV and the AO index is largest in this month. Inversion of a PV anomaly results in a wind anomaly and a static stability anomaly, both of which affect baroclinic instability in the troposphere. We examine the differences in the degree of baroclinic instability between winter months with a strong positive average AO index and winter months with a strong negative average AO index. Furthermore, the influence of variations in the static stability on the Rossby scale height are presented, to estimate its effect on the downward influence of stratospheric PV anomalies on the wind field.

Section 2 gives an overview of the dataset that has been used. The PV inversion equation is introduced in section 3. The differences in wind and PV between the two AO phases and the influence of variations in the static stability on the difference in PV are presented in section 4. The solutions of the PV inversion equation that provide an answer to the question of how stratospheric PV anomalies affect the tropospheric wind and baroclinic instability are discussed in section 5. Finally, conclusions are given in section 6.

2. Data

The European Centre for Medium-Range Weather Forecasts (ECMWF) ERA-40 reanalysis dataset is used. The monthly mean January ERA-40 data of the zonal wind and the temperature for the 1958–2002 period are interpolated from isobaric to isentropic levels by the method described by Edouard *et al.* (1997). In order to make optimal use of the available ERA-40 data, a stretched grid in the vertical direction is employed. Zonal averaging and averaging over the whole 45 yr period gives a climatological dataset of zonal and January mean zonal wind and pressure on isentropic levels. The climatological isentropic potential vorticity Z_θ (Hoskins *et al.*, 1985) is then calculated from

$$Z_\theta = \frac{\zeta_\theta + f}{\sigma}. \tag{1}$$

Here ζ_θ is the zonal mean isentropic relative vorticity, f is the Coriolis parameter and σ is the zonal mean isentropic density:

$$\zeta_\theta = -\frac{1}{a}\frac{\partial u}{\partial \phi} + \frac{u \tan \phi}{a}, \tag{2}$$

$$\sigma = -\frac{1}{g}\frac{\partial p}{\partial \theta}. \tag{3}$$

Here u is the zonal wind, a is the radius of the Earth, ϕ is the latitude, p is the pressure, θ is the potential temperature and g is the gravitational acceleration. The domain of this dataset ranges from 90°N to 10°N in the horizontal, with a resolution of 2.5°, and from the Earth's surface to about 1600 K in the vertical, with a resolution varying from 3.4 K near the surface to about 20 K in the upper layers. We assume that the potential temperature of the Earth's surface coincides with the temperature of the 1000 hPa level. The lower boundary (also referred to as 'the surface') is defined as the lowest level of the grid that is above the Earth's surface. The potential temperature of the lower boundary thus varies with latitude, from 250 K at 90°N to about 300 K at 10°N. By putting the southern boundary well north of the Equator, we avoid the problems associated with the inversion (see section 3) of negative values of potential vorticity that are found near the Equator.

3. The potential vorticity inversion equation

To study the relation between the potential vorticity and the zonal wind, we derive a PV inversion equation that is based on the invertibility principle (Kleinschmidt, 1950; Hoskins *et al.*, 1985), which states that, together with suitable

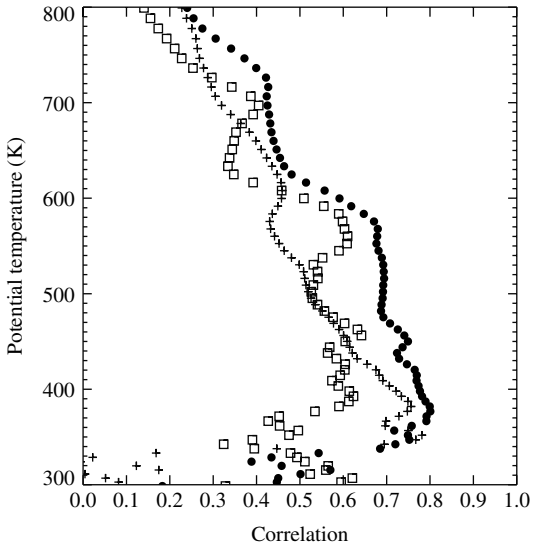

Figure 1. Correlation between the AO index and the polar cap PV as a function of potential temperature (K) for years with an AO index larger than 0.5 or smaller than −0.5 times the standard deviation of all the AO index values. Monthly mean values for December (squares), January (solid dots) and February (plus symbols).

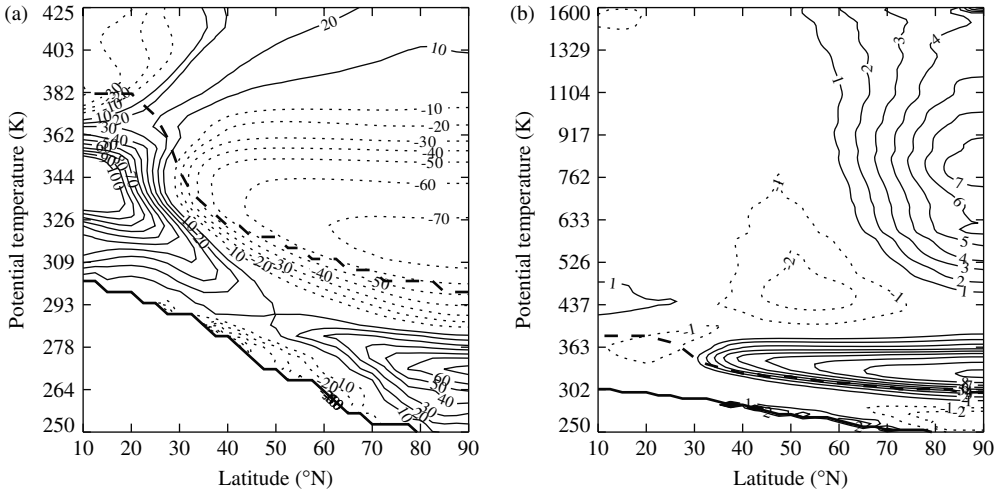

Figure 2. (a) The deviation from the reference state of the isentropic density, as a percentage of the reference isentropic density, $(\sigma')/\sigma_{\mathrm{ref}} \times 100\%$, and (b) the deviation from the reference state of the scaled PV, Z'_θ (in PVU). The fields are plotted as a function of potential temperature (K) and latitude (°N) (note the different scales on the vertical axes). The contour interval is 10% for (a) and 1 PVU for (b), with the zero lines omitted and negative values indicated by thin dashed lines. The thick line near the lower boundary of the domain indicates the surface and the thick dashed line the tropopause (which is defined as the 2 PVU isopleth).

boundary conditions, the PV determines all other dynamical fields. We assume axisymmetry about the North Pole. The PV inversion equation is derived from the definition of the isentropic potential vorticity (Eq. (1)). We simply define the time mean (indicated by a bar) and zonal mean (indicated by square brackets) potential vorticity as follows (neglecting deviations from the zonal average):

$$[\overline{Z_\theta}] = \frac{[\overline{\zeta_\theta}] + f}{[\overline{\sigma}]}. \tag{4}$$

The time and zonal mean zonal wind is assumed to be in hydrostatic balance and in gradient wind balance with the time and zonal mean temperature and pressure (again neglecting deviations from the zonal average), i.e.

$$\frac{\partial[\overline{\Psi}]}{\partial\theta} = [\overline{\Pi}] \tag{5}$$

and

$$[\overline{u}]\left(f + \frac{[\overline{u}]\tan\phi}{a}\right) = -\frac{1}{a}\frac{\partial[\overline{\Psi}]}{\partial\phi}. \tag{6}$$

In these equations Π is the Exner function ($= c_{\mathrm{p}}T/\theta$, with c_{p} the heat capacity of dry air at constant pressure and T the temperature) and Ψ is the isentropic stream function ($\Psi = c_{\mathrm{p}}T + gz$, with z the height).

Differentiation of Eq. (4) with respect to ϕ, using Eqs (5) and (6) and the equation of state, leads to the PV inversion equation. Dropping the averaging symbols, this equation is

$$\frac{Z_\theta}{g}\frac{\partial}{\partial\theta}\left(\rho\theta f_{\mathrm{loc}}\frac{\partial u}{\partial\theta}\right) + \frac{\partial^2 u}{\partial r^2} + \frac{\tan\phi}{a}\frac{\partial u}{\partial r} - \frac{u}{a^2\cos^2\phi} = \sigma\frac{\partial Z_\theta}{\partial r} - \frac{\partial f}{\partial r}, \tag{7}$$

with

$$\left.\begin{aligned} f_{\mathrm{loc}} &= f(r) + \frac{2\tan\phi}{a}u, \\ r &= a\left(\frac{\pi}{2} - \phi\right), \\ f(r) &= 2\Omega\sin\phi = 2\Omega\cos\left(\frac{r}{a}\right). \end{aligned}\right\} \tag{8}$$

Here, r is the distance from the Pole measured along the surface of the Earth, ρ is the density and Ω is the rotation rate of the Earth.

The PV inversion equation (Eq. (7)) can be seen as the formulation of thermal wind balance in terms of potential vorticity. It describes the flow pattern that is associated with a specific pattern of the potential vorticity in a balanced axisymmetric vortex centred at the Pole.

The boundary condition at $r = 0$ is simply that $u = 0$, because the vortex is assumed to be axisymmetric and centred at the Pole. At the outer boundary at 10°N we prescribe the wind according to the circulation theorem (Hoskins *et al.*, 1985, p 897). At the upper boundary we impose the average wind of the specific months we are considering. At the lower boundary, thermal wind balance is imposed, which is approximated in isentropic coordinates by

$$\frac{\partial u}{\partial\theta} = \frac{c_{\mathrm{p}}}{f_{\mathrm{loc}}\theta}\frac{\partial T}{\partial r}. \tag{9}$$

The temperature at the lower boundary is derived from the zonal mean pressure on isentropic levels. The influence of the lower boundary condition (also referred to as the 'surface boundary condition') on the inverted winds is examined in section 5.

4. The Arctic Oscillation and potential vorticity

In this section the relation between the PV and the AO index is studied. For this study the monthly AO index from the National Centers for Environmental Prediction/National Center for Atmospheric Research (NCEP/NCAR) reanalysis is used (Thompson and Wallace, 2000). This index is defined as the leading empirical orthogonal function (EOF) of sea-level pressure poleward of 20°N. It is based on the period 1958–1997, which is close to the period we examine (1958–2002). A particular January month is defined as having a positive (negative) AO index if its average AO index is larger than (smaller than) plus (minus) 0.5 times the standard deviation of all the AO index values (this will be referred to as the 'AO criterion'). With the AO criterion,

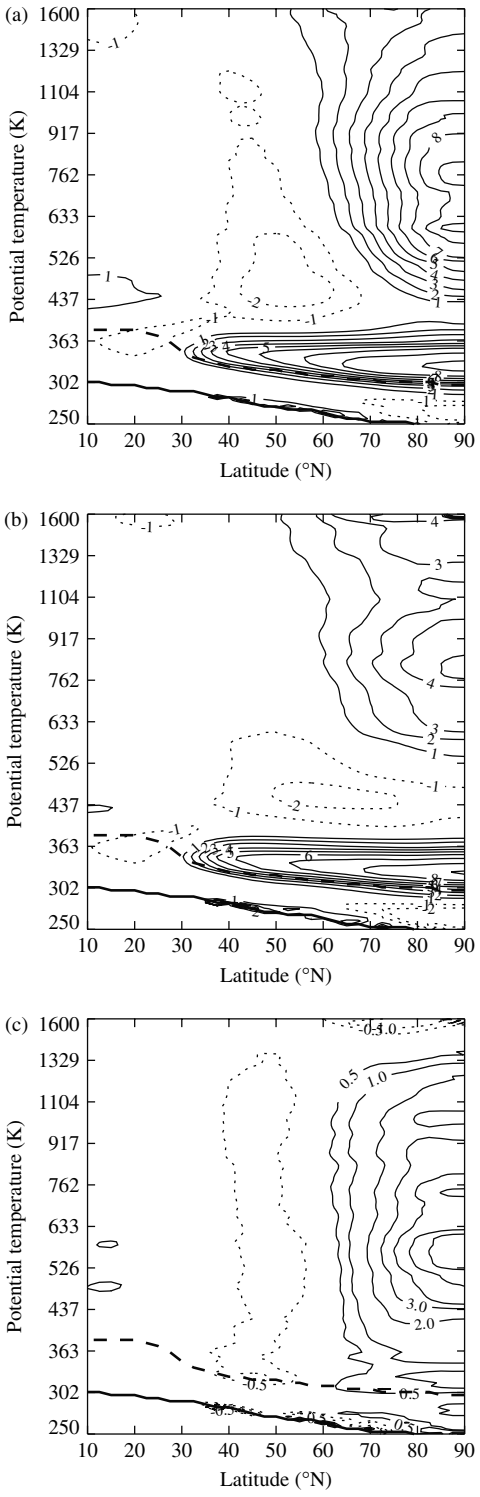

Figure 3. Scaled Z'_θ (in PVU) for (a) the positive AO case, (b) the negative AO case and (c) the positive–negative AO case. Contours as in Figure 2(b); for (c) the ±0.5 PVU contour is also added.

the following 15 years with a positive AO index for January have been determined: 1962, 1964, 1973, 1975, 1981, 1983, 1984, 1988, 1989, 1990, 1991, 1992, 1993, 2000 and 2002, and the following 11 years with a negative AO index have been identified: 1959, 1960, 1963, 1966, 1969, 1970, 1977, 1979, 1980, 1985 and 1998.

The January mean PV is determined for all years (1958–2002) from the January and zonal mean u and p fields. The same is done for the months of December (1957–2001) and February (1958–2002). The correlation between the AO index and the polar cap PV (average area-weighted PV north of 70°N) for the winter months is shown in Figure 1 for the years that satisfy the AO criterion. There is a clear positive correlation between the AO index and the polar stratospheric PV. The correlation is largest in January, where it is larger than 0.6 in the lower stratosphere, between about 350 K and 600 K. This relation between the AO index and stratospheric PV does not present information about cause and effect, but it indicates that changes in the stratospheric PV are related to changes in the AO index. Based on this relation, we expect a different stratospheric PV distribution for January months with a positive AO index than for January months with a negative AO index. PV inversion will be used to examine the influence of the stratospheric PV on the tropospheric winds, to see whether stratospheric PV is associated with the winds in a similar way as the AO index. The results presented in the rest of the article are for January.

The zonal mean PV and the isentropic density are split into a reference state and an anomaly as follows:

$$\left.\begin{aligned} Z_\theta &\equiv Z_{\theta,\mathrm{ref}} + Z'_\theta, \\ \sigma &\equiv \sigma_{\mathrm{ref}} + \sigma', \end{aligned}\right\} \tag{10}$$

with

$$Z_{\theta,\mathrm{ref}} = \frac{f}{\sigma_{\mathrm{ref}}} \tag{11}$$

and

$$\sigma_{\mathrm{ref}} = \frac{\int \sigma a \cos(\phi)\, \mathrm{d}\phi}{\int a \cos(\phi)\, \mathrm{d}\phi}. \tag{12}$$

In other words, the reference isentropic density σ_{ref} is the area-weighted average of σ over the domain in question. In our case this is the area poleward of 10°N. Therefore, σ_{ref} depends only on the height (θ). The PV anomaly, Z'_θ, represents that part of the PV field that induces a wind field, according to the PV inversion equation (Eq. (7)).

Figure 2(a) shows that $\sigma'/\sigma_{\mathrm{ref}}$ is quite large (up to ± 70%) in the troposphere and in the polar lower stratosphere. Values are only shown up to 425 K, because σ' decreases to values of less than 20% of σ_{ref} in most of the domain above 425 K. The large latitudinal variations in the static stability in the UTLS region have important implications for the influence of stratospheric PV anomalies on the troposphere, since the depth at which the influence of a PV anomaly is felt is proportional to σ. An overestimation of σ will lead to an overestimation of the influence of the stratospheric PV anomaly on the tropospheric winds.

Figure 2(b) shows the January climatological Z'_θ field in PVU (1 PVU = 10^{-6} K m^2 kg^{-1} s^{-1}), where for plotting purposes, the PV is multiplied by a scaling factor $(\theta/\theta_0)^{-9/2}$ (Lait, 1994), with $\theta_0 = 380$ K. We see two distinct positive PV anomalies: one broad, flat anomaly near the tropopause, below 425 K, that extends from the Pole to the Subtropics, and one more narrow, tall anomaly in the polar stratosphere, above 425 K, that only extends from the Pole to about 60°N. We will refer to the former anomaly as the 'UTLS PV anomaly'. The latter anomaly will be referred to as the 'stratospheric polar cap PV anomaly'.

The average distributions of the January PV anomaly for the positive AO case, the negative AO case and the

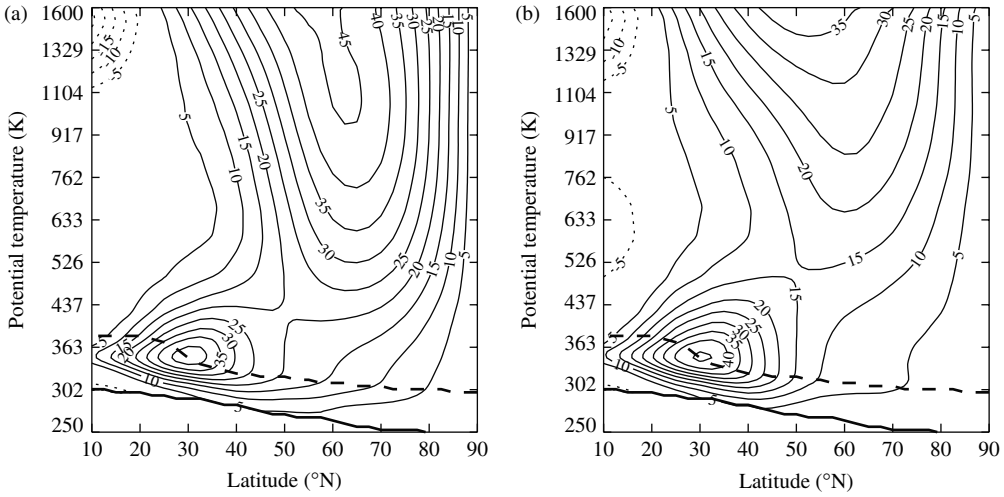

Figure 4. January mean zonal mean zonal wind (in m s^{-1}), derived from the ERA-40 dataset, for (a) the positive AO case and (b) the negative AO case. Contours are every 5 m s^{-1}, the zero line is omitted and negative values are indicated by thin dashed lines.

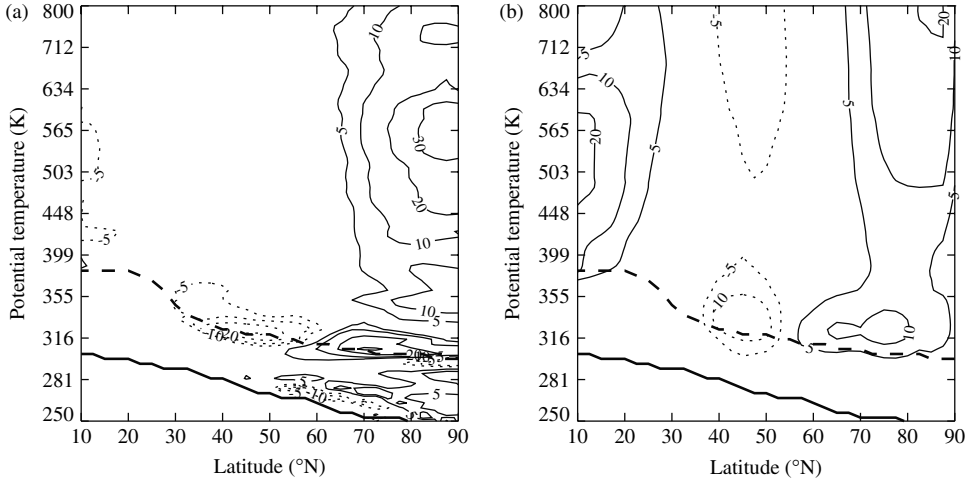

Figure 5. The difference in scaled Z'_θ between the positive and negative AO cases as a percentage of the climatological reference scaled PV for calculation of the PV with (a) ζ held at its climatological value and (b) σ held at its climatological value. Contours at $\pm$ 5%, 10% and then every 10%.

difference between the positive and negative AO case are plotted in Figure 3(a), (b) and (c), respectively. The positive and negative AO case values are determined from the corresponding mean u and p fields, where the mean is taken over the January months that obey the AO criterion. Clearly, the stratospheric polar cap PV anomaly is larger in amplitude and extends further downward when the AO is in the positive phase. The amplitude of the UTLS PV anomaly is slightly stronger between 40°N and 50°N in the negative AO phase. This leads to a larger meridional PV gradient in the Subtropics if the AO index is negative, resulting in a stronger subtropical jet (see section 5). Nevertheless, the UTLS PV anomaly has a slightly larger amplitude over the Pole if the AO index is positive. The zonal mean zonal wind averaged over the specific January months that satisfy the AO criterion is shown for the positive and negative AO cases in Figure 4(a) and (b), respectively. The observed subtropical jet is indeed stronger for the negative AO case. However, the polar night stratospheric jet is much stronger in the positive AO phase.

It is interesting to examine which part of the difference in PV as shown in Figure 3(c) is related to variations in the relative vorticity, and which part is related to variations in the static stability. To study this, the PV is calculated twice for both the positive and negative AO cases: firstly the climatological relative vorticity is used, to study the influence of variations in σ, and secondly the climatological static stability is used, to study the influence of variations in ζ. The contributions to the PV anomaly difference are shown in Figure 5(a) and (b) for the static stability and relative vorticity, respectively. The contributions are given as a percentage of the climatological reference PV field to make comparison of different isentropic levels easier. Between 600 K and 800 K, variations in static stability and relative vorticity both contribute to the PV anomaly difference, by about equal amounts, while below 600 K the static stability contribution dominates. In the UTLS region the influence of static stability variations on the PV anomaly difference is about +20% of the climatological reference PV from mid- to high latitudes and −20% in the Subtropics, compared with influences of the same sign of about 5–10% for the relative vorticity contributions. This indicates that the variations in the static stability to a large degree determine the difference in the UTLS PV anomaly between positive and negative AO cases. Black (2002) does not take these static stability variations into account, and therefore considers only the part that is related to variations in the relative vorticity (Figure 5b). We consider the total PV difference,

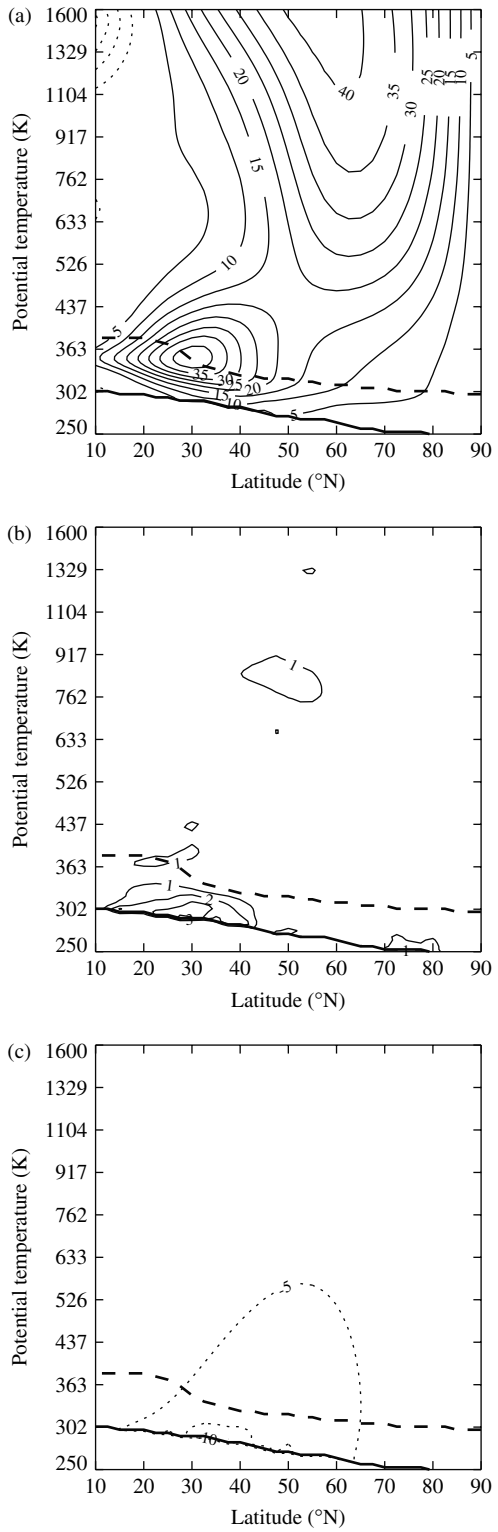

Figure 6. (a) Wind ($m\,s^{-1}$) obtained from inverting the ERA-40 zonal mean PV field for January. (b) Inverted minus ERA-40 wind ($m\,s^{-1}$) for January. (c) Wind ($m\,s^{-1}$) obtained from inverting the ERA-40 zonal mean reference PV field for January and imposing thermal wind balance at the lower boundary. The contour interval is 5 $m\,s^{-1}$ for (a) and (c) and 1 $m\,s^{-1}$ for (b), zero lines are omitted and negative values are indicated by thin dashed lines.

and PV inversion will result in a static stability anomaly as well as a wind anomaly. In section 5 we will examine how variations in the static stability affect the Rossby scale height.

5. Effect of stratospheric PV on tropospheric winds

Equation (7) is solved, by successive relaxation, for the climatological PV as derived from the zonal mean and time mean (1958–2002) January u and p ERA-40 fields. The resulting 'inverted wind field' (Figure 6(a)) is compared with the ERA-40 wind field and the difference is shown in Figure 6(b). The differences between the ERA-40 wind and the inverted wind are very small in most of the domain. Differences of up to 3 $m\,s^{-1}$ occur near the surface in the Subtropics, indicating that thermal wind balance might not be valid in these regions.

Figure 6(c) shows the wind field that is obtained from inverting the reference PV, with zero wind as boundary condition at the Pole, at 10°N and at the top of the domain, but imposing a thermal wind (Eq. (9)) at the lower boundary. Since the reference PV does not induce a wind field, the resulting wind is the influence of the lower boundary condition on the wind field. This means that if the variation with latitude of the temperature at the lower boundary were not taken into account, the subtropical to midlatitude wind speeds in the troposphere and lower stratosphere would be higher by 5–10 $m\,s^{-1}$. The surface boundary condition thus cancels part of the influence that the PV field has on the wind.

The PV anomaly fields shown in Figure 3 are now split into two parts: the UTLS PV anomaly that extends from the surface to 425 K and the stratospheric polar cap PV anomaly that extends from 425–1600 K (425 K $\sim$ 17 km, 1600 K $\sim$ 40 km). Both PV anomalies are inverted separately (with the reference PV as a background state), for both the positive and negative AO cases. The results are shown in Figures 7 and 8 for the positive and negative AO cases, respectively. The boundary condition at 10°N is zero wind outside the area of the PV anomaly (which is the same as determined with the circulation theorem when the reference PV and static stability are used). At the upper boundary, we again impose the average ERA-40 wind of the specific months we are considering for the stratospheric polar cap PV anomaly. The wind at the upper boundary is set to zero for the UTLS PV anomaly. At the lower boundary a realistic thermal wind (according to Eq. (9)) is imposed for the UTLS PV anomaly, while zero thermal wind at the surface is imposed for the stratospheric polar cap PV anomaly. The surface temperature distribution is thus taken together with the PV anomaly that borders the surface. Figures 7(a) and 8(a) show that the subtropical jet can be attributed to the UTLS PV anomaly. This PV anomaly also affects the vertical wind shear in the midlatitude troposphere and affects the stratospheric winds up to the middle stratosphere from the Subtropics to the high latitudes. Figures 7(b) and 8(b) show that the stratospheric polar cap PV anomaly is needed to explain the high wind speeds in the polar vortex, and that it mainly affects the midlatitude winds in the stratosphere itself. For the positive AO case (Figure 7(b)) there is also some influence on the winds in the extratropical troposphere, in agreement with Black (2002) and Ambaum and Hoskins (2002). For the negative AO case (Figure 8(b)), the wind speeds in the lower stratosphere are reduced compared with the positive AO case or the climatology.

Inversion of the tropospheric part of the UTLS PV anomaly (surface to tropopause), imposing a thermal wind at the lower boundary (Eq. (9)), indicates that most of the subtropical jet is induced by this PV anomaly. This

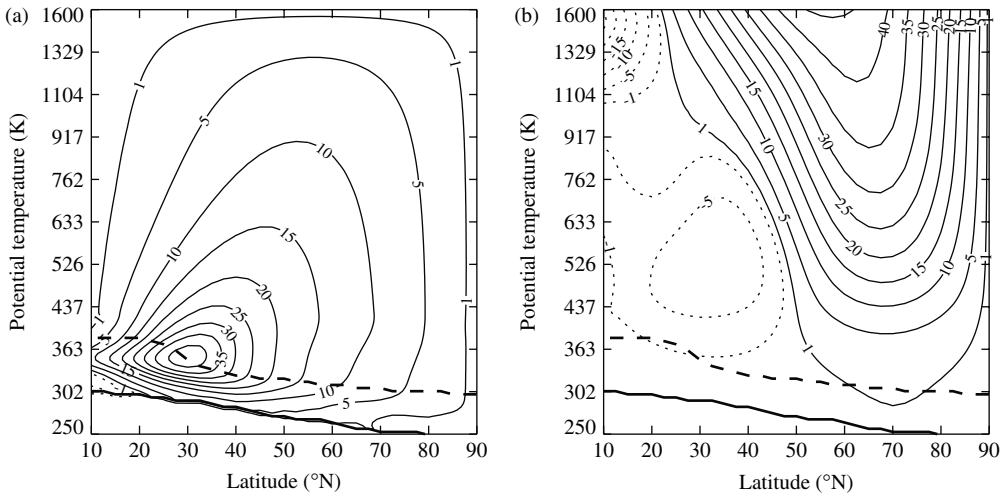

Figure 7. Inverted wind ($m\,s^{-1}$) for the positive AO case, obtained from inverting the PV field with a non-zero part of the PV anomaly (a) between the surface and 425 K (UTLS PV anomaly) and (b) between 425 K and 1600 K (stratospheric polar cap PV anomaly). Contours are as in Figure 4, and a $1\,m\,s^{-1}$ contour is added.

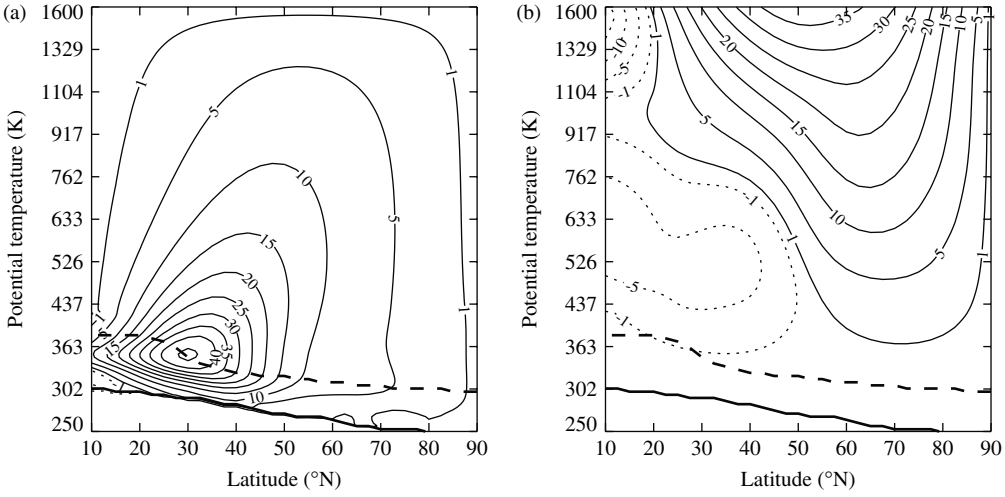

Figure 8. Same as Figure 7, but for the negative AO case.

PV anomaly has a negative influence on the mid- to high latitude winds in the troposphere, mainly due to the effect of the surface boundary condition. For the inversion of the stratospheric part of the UTLS PV anomaly (defined as that part that lies above the PV = 2 PVU isopleth), zero thermal wind ($\partial u/\partial\theta = 0$) is imposed at the lower boundary. This PV anomaly influences the wind from the Subtropics to high latitudes and from the surface to the middle stratosphere.

Figure 9 presents the difference in inverted wind between the positive and negative AO cases with a PV anomaly over the whole domain (Figure 9(a)), a PV anomaly above 425 K (Figure 9(b)) and a PV anomaly between the tropopause and 425 K (Figure 9(c)) (the small differences at the lower boundary in Figure 9(c) are related to the discretization of the boundary; since these effects are only small they do not affect the general conclusions). The ERA-40 wind difference between positive and negative AO cases is very similar to the inverted difference given in Figure 9(a) (with differences smaller than $1\,m\,s^{-1}$ over most of the domain). Furthermore, the sum of the inverted winds from the separate PV anomalies is about the same as the inverted wind from the sum of the PV anomalies, despite the nonlinearity of the inversion. Figure 9(b) shows that the stratospheric polar cap PV anomaly difference is related to a tropospheric wind difference of about $0.5\,m\,s^{-1}$ from the mid- to high latitudes. The difference in the stratospheric part of the UTLS PV anomaly has a similar effect on the surface wind difference, but a larger effect on the upper troposphere of about $1\,m\,s^{-1}$ and up to $3\,m\,s^{-1}$ in the lower stratosphere between 60°N and 70°N (Figure 9(c)). The difference between positive and negative AO cases in the upper tropospheric vertical wind shear at midlatitudes can thus partly be attributed to the difference in stratospheric PV. This is mainly caused by the stratospheric part of the UTLS PV anomaly.

So far, the temperature structure at the lower boundary has been taken into account together with the (tropospheric part of the) UTLS PV anomaly. To examine the influence of the lower boundary condition on the inverted wind difference between positive and negative AO cases, the inversions that led to Figure 9(a) have been repeated with the climatological lower boundary condition. The climatological surface temperature is thus used for the inversion of both AO cases, instead of the surface temperatures that correspond to the positive and negative AO cases. Figure

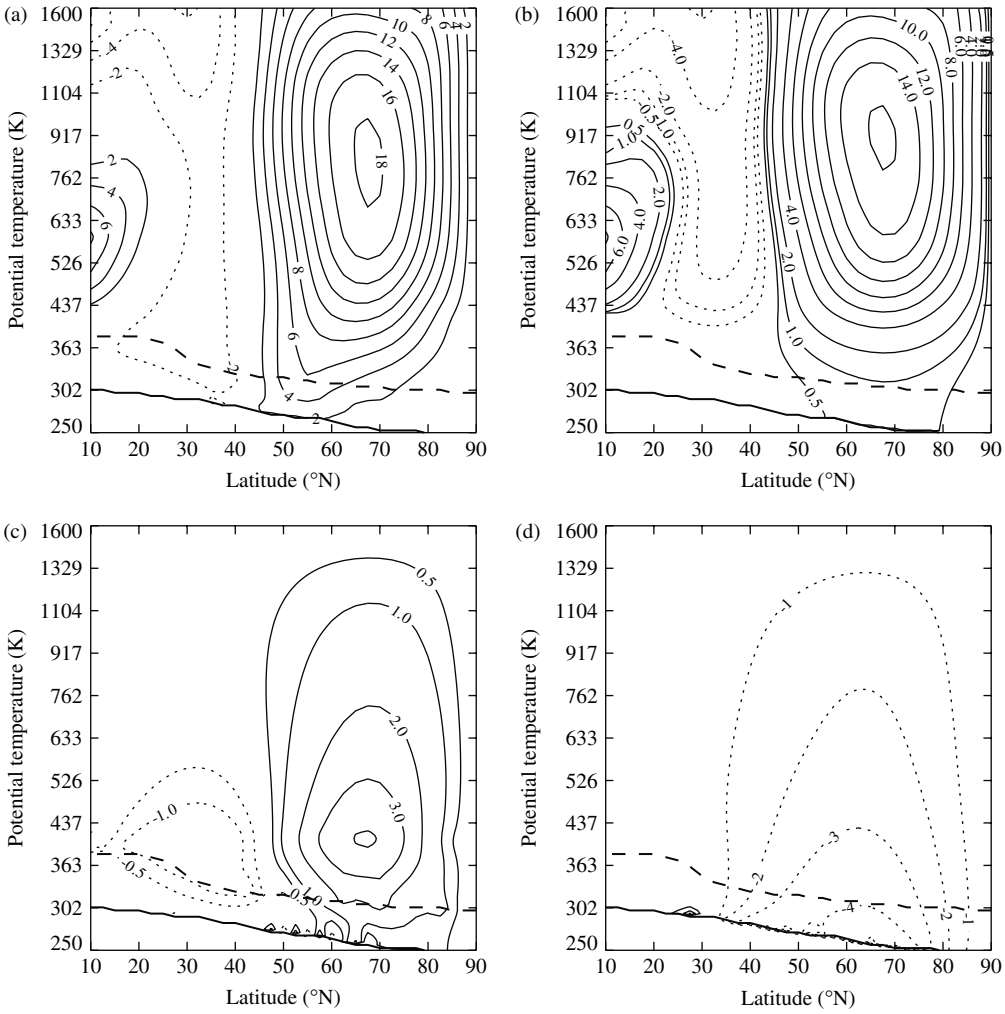

Figure 9. Difference in inverted wind (m s^{-1}) (positive–negative AO case), obtained from inverting the PV field with a non-zero part of the PV anomaly (a) in the total domain, (b) between 425 K and 1600 K (stratospheric polar cap PV anomaly) and (c) between the tropopause and 425 K (stratospheric part of the UTLS PV anomaly). (d) Influence of the variations in surface temperature (positive–negative AO case) on the inverted wind difference, compared with results using the climatological surface temperature distribution for both the positive and negative AO cases (see text for further explanation). Contours are every 2 m s^{-1} for (a) and (b), with $\pm$ 0.5 and $\pm$ 1 m s^{-1} contours added for (b), and every 1 m s^{-1} for (c) and (d) with a $\pm$ 0.5 contour added for (c). Zero lines are omitted and negative values are indicated by thin dashed lines.

9(d) shows the difference compared with using realistic boundary conditions. The difference in surface temperature between positive and negative AO cases thus decreases the inverted wind difference by the amount displayed in Figure 9(d). This means that use of the climatological surface boundary condition would clearly overestimate the wind difference. So in order to explain fully the observed wind differences between the positive and negative AO cases by means of PV inversion, the difference in surface temperature between the two AO cases needs to be taken into account.

The vertical wind shear in the troposphere at midlatitudes is much larger for the positive AO case than for the negative AO case (Figure 4). The vertical wind shear is important for baroclinic instability and cyclogenesis. As a measure of baroclinicity b we use the Eady growth rate (Hoskins and Valdes, 1990):

$$b = \frac{0.31f\left|\dfrac{\partial u}{\partial z}\right|}{N}, \tag{13}$$

with N the Brunt–Väisälä frequency, which is proportional to the square root of the static stability (and the static stability is proportional to the inverse of σ).

Since the stratospheric polar cap PV anomaly hardly influences the tropospheric winds, we only examine the baroclinicity that is related to the UTLS PV anomaly. Figure 10 demonstrates that the baroclinic growth rate between 50°N and 70°N is greater for the positive AO cases than for the negative AO cases throughout the full depth of the troposphere. It is indeed observed that more and deeper cyclones are formed during January months with a positive AO index than during January months with a negative AO index (Sickmöller *et al.*, 2000). The stronger Equator-to-Pole heat transport associated with the more numerous or stronger cyclones might explain an important part of the higher midlatitude temperatures during winter months with a positive AO index compared with winter months with a negative AO index. Our results agree with those of Wittman *et al.* (2007), who found that shear in the lower stratosphere affects baroclinic development, and that a higher shear is associated with a higher than normal tropospheric Northern Annular Mode (NAM) index (the NAM index is similar to the AO index).

Figure 5 showed that part of the PV anomaly field is related to differences in the static stability between the positive and

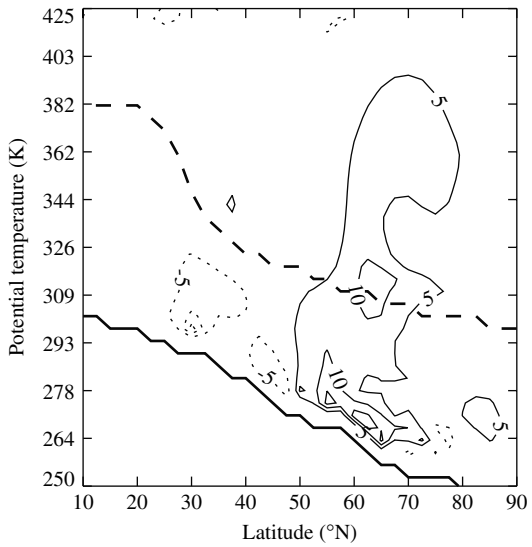

Figure 10. January mean measure of the baroclinicity or Eady growth rate (in s^{-1}) for the positive AO case minus the negative AO case, derived from the wind field and static stability resulting from the inversion of the UTLS PV anomaly. Contours are in units of $10^{-7}\,s^{-1}$ with a contour interval of $5 \times 10^{-7}\,s^{-1}$ (zero lines omitted).

negative AO cases. The change of wind shear and static stability during the PV inversion are coupled, therefore it is not possible to examine the separate influences on the baroclinicity. It is, however, possible to study the influence of variations in the static stability on the Rossby scale height, which is a measure of the depth at which the influence of a PV anomaly is felt. The Rossby scale height is proportional to the inverse of the Brunt–Väisälä frequency, and is calculated for both AO cases with only variations in N taken into account and other factors held at their climatological value. In the mid- to high latitude tropopause region the difference in Rossby scale height (positive AO–negative AO) is about −5% of the climatological Rossby scale height, or of the order of −500 m. This means that neglecting variations in the static stability would underestimate the influence of the stratospheric part of the UTLS PV anomaly on the tropospheric winds for the negative AO case compared with the positive AO case, and thus overestimate the difference between the cases. This explains the results of Black (2002), who does not take variations in static stability into account and indeed finds a somewhat larger influence of the stratospheric PV on the tropospheric winds than we find in the present study.

6. Conclusion

In this article, the connection between the average AO index in January and the January average zonal mean potential vorticity (PV) distribution in the Northern Hemisphere is studied. Using nonlinear PV inversion, we determine the large-scale zonal mean adjustment to amplitude variations in the monthly average zonal mean potential vorticity that are associated with the Arctic Oscillation. By defining the PV anomaly as that part of the PV that induces a wind, we identify two separate positive PV anomalies in the Northern Hemisphere (centred over the North Pole), i.e. a relatively broad and shallow PV anomaly in the upper troposphere and lower stratosphere and a relatively tall PV anomaly higher in the stratosphere (above 425 K). The amplitude of the latter PV anomaly is much larger during January months with a positive AO index than during January months with a negative AO index. According to the solution of the PV inversion equation, the influence on the wind of the latter PV anomaly is largest in the stratosphere, but can also explain a small part of the difference in mid- to high latitude tropospheric wind between January months with a positive AO index and January months with a negative AO index. These results are in agreement with those of Black (2002) and also with the ideas presented by Ambaum and Hoskins (2002). The present study elaborates on the findings of Black (2002) and Ambaum and Hoskins (2002) by investigating the influence of the higher stratospheric PV and lower stratospheric PV separately, and we conclude that it is mainly the lower stratospheric PV that affects the tropospheric winds.

We find that by far the largest part of the monthly variability in the tropospheric zonal mean zonal wind that accompanies the variations in the monthly mean AO index is induced by the variability in the amplitude and form of the UTLS PV anomaly. In the lower stratosphere and upper troposphere, the static stability deviates substantially from the latitude-independent reference state. According to the solution of the PV inversion equation, the UTLS PV anomaly influences the vertical wind shear as well as the static stability at midlatitudes, leading to a larger than average degree of baroclinic instability at midlatitudes when the AO index is positive. This is a possible explanation for the observed higher than average frequency of intense midlatitude cyclones during winter months with an average positive AO index.

We conclude that the zonal mean dynamical impact of the stratosphere on the troposphere can be described by a large-scale adjustment to amplitude variations in the zonal mean stratospheric PV distribution. This conclusion seems to disagree with the conclusion of Charlton *et al.* (2005), who state that 'the dynamical impact of the stratosphere on the troposphere cannot be described by large-scale adjustment to the stratospheric PV distribution'. The apparent inconsistency is routed in the fact that Charlton *et al.* (2005) do not investigate the effect of amplitude variations in the zonal mean stratospheric PV distribution, but only investigate the effect of zonal asymmetries in the stratospheric PV distribution.

The marked difference between the positive AO phase and the negative AO phase in the amplitude of the PV anomaly above 425 K is probably associated with meridional mixing or displacement of potential vorticity when Rossby waves, which propagate upwards from the troposphere, break in the stratosphere, especially during sudden stratospheric warming events, such as in January 1985. The question of what determines the differences between the positive AO phase and the negative AO phase in the amplitude and form of the UTLS PV anomaly is open, but we hypothesize that the intensity of the hydrological cycle in the Tropics and wave breaking near the tropopause (the formation of cut-off lows and blocking highs) in the latitude band between approximately 30°N and 70°N both play a role.

Acknowledgements

The ECMWF ERA-40 data used in this study have been provided by ECMWF. The AO-related dataset that is used has been provided by the Climate Explorer

website (http://climexp.knmi.nl/selectindex.cgi?someone@somehere).

References

Ambaum MHP, Hoskins BJ. 2002. The NAO troposphere–stratosphere connection. *J. Climate* **15**: 1969–1978.

Baldwin MP, Dunkerton TJ. 1999. Propagation of the Arctic Oscillation from the stratosphere to the troposphere. *J. Geophys. Res.* **104**(D24): 30937–30946.

Baldwin MP, Dunkerton TJ. 2001. Stratospheric harbingers of anomalous weather regimes. *Science* **294**: 581–584.

Black RX. 2002. Stratospheric forcing of surface climate in the Arctic Oscillation. *J. Climate* **15**: 268–277.

Charlton AJ, O'Neill A, Berrisford P, Lahoz WA. 2005. Can the dynamical impact of the stratosphere on the troposphere be described by large-scale adjustment to the stratospheric PV distribution? *Q. J. R. Meteorol. Soc.* **131**: 525–543.

Davis CA. 1992. Piecewise potential vorticity inversion. *J. Atmos. Sci.* **49**: 1397–1411.

Edouard S, Vautard R, Brunet G. 1997. On the maintenance of potential vorticity in isentropic coordinates. *Q. J. R. Meteorol. Soc.* **123**: 2069–2094.

Hartley DE, Villarin JT, Black RX, Davis CA. 1998. A new perspective on the dynamical link between the stratosphere and troposphere. *Nature* **391**: 471–474.

Hartmann DL, Wallace JM, Limpasuvan V, Thompson DWJ, Holton JR. 2000. Can ozone depletion and global warming interact to produce rapid climate change? *PNAS* **97**(4): 1412–1417.

Hoskins BJ, Valdes PJ. 1990. On the existence of storm-tracks. *J. Atmos. Sci.* **47**(15): 1854–1864.

Hoskins BJ, McIntyre ME, Robertson AW. 1985. On the use and significance of isentropic potential vorticity maps. *Q. J. R. Meteorol. Soc.* **111**: 877–946.

Kleinschmidt E. 1950. Über aufbau und entstehung von zyklonen. *Meteorologische Rundschau* **3**(Heft 1/2): 1–6.

Lait LR. 1994. An alternative form for potential vorticity. *J. Atmos. Sci.* **51**(12): 1754–1759.

Sickmöller M, Blender R, Fraedrich K. 2000. Observed winter cyclone tracks in the northern hemisphere in re-analysed ECMWF data. *Q. J. R. Meteorol. Soc.* **126**: 591–620.

Thompson DWJ, Wallace JM. 1998. The Arctic Oscillation signature in the wintertime geopotential height and temperature fields. *Geophys. Res. Lett.* **25**(9): 1297–1300.

Thompson DWJ, Wallace JM. 2000. Annular modes in the extratropical circulation. Part I: Month-to-month variability. *J. Climate* **13**: 1000–1016.

Wittman MAH, Charlton AJ, Polvani LM. 2007. The effect of lower stratospheric shear on baroclinic instability. *J. Atmos. Sci.* **64**: 479–496. DOI:10.1175/JAS3828.1.

